

1 **Supplementary information**

2

3

4 Long-term trends in wild-capture and population dynamics point to an
5 uncertain future for captive elephants.

6

7

8

9

10

11

12

13

14

15

16

17

18

19

20 **S1. Data selection**

21 The data recorded for all registered elephants includes: identification number and name, birth
22 origin (captive-born or wild-caught), date and place of birth, mother's identification number and
23 name, year and place of capture (if wild-captured), year or age of taming, identities of all calves
24 born, date of death or last known date alive, and cause of death. The initial studbook contained
25 data from 1876 to 2014. Further restrictions to the studbook were made because only sparse
26 records were available until the 1950s. Therefore, only females born after 1920 if captive-born
27 were included, and both mortality and birth records for females present in the population before
28 1960 were discarded. Records for wild-caught individuals were incomplete before 1951 and age
29 estimates for wild-caught elephants may have lower accuracy after the individuals have achieved
30 full body height (at the age of 25 years in this working population) (Mumby et al. 2015). Therefore,
31 only wild-caught females entering the population after 1951 and caught before the age of 25
32 (~70% of those captured), were included here to increase the reliability of our age-specific
33 mortality and fertility estimates. Thus, our measure of annual wild-capture rate does not reflect
34 the total number of individuals caught from the wild each year, but instead general trends of wild-
35 capture through time in Myanmar. Nevertheless, the majority of wild-caught elephants were below
36 an estimated age of 25 at capture: during 1951-1999 the median age at capture varied between
37 8 and 13 years, depending on the method of capture (Lahdenperä et al. 2018), and capturers
38 generally targeted young, healthy-looking individuals which were easier to train than older ones.
39 There was also a female bias in wild-capture, who comprised 60% of wild-caught individuals in
40 the initial studbook. Finally, individuals with erroneous or discontinuous death/departure/birth
41 information were removed (5% of elephants). The final studbook was a female-only dataset (N =
42 3585, wild-caught = 1215) with individuals from 11 out of the 14 regional divisions of Myanmar,
43 of which 2117 were censored. This female-only dataset was used in all subsequent analyses.

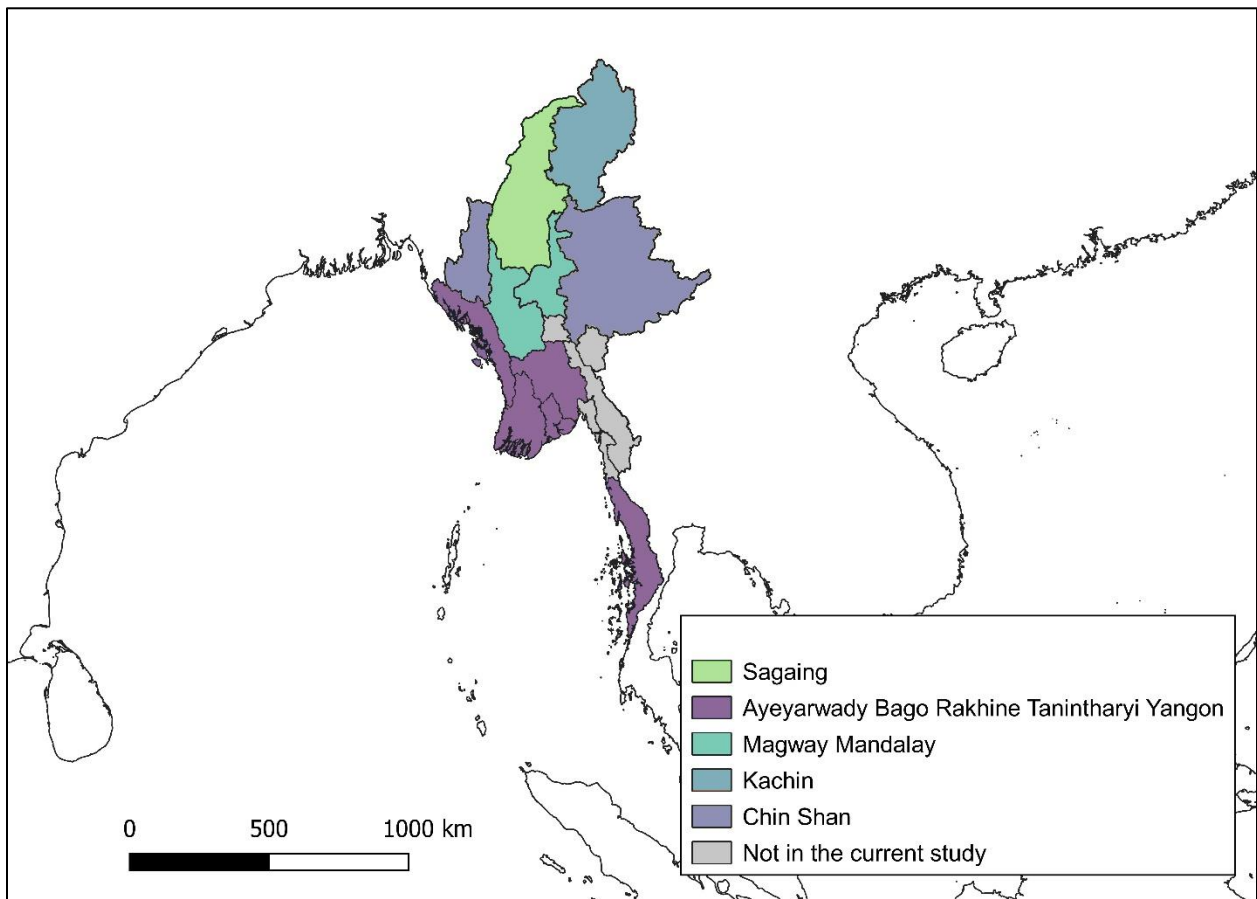
45 **S2. Model selection**

46 We used model selection in order to explore the fit of linear and non-linear explanatory variables
47 on female birth and mortality rates, as well as on the interaction between age, year and birth origin
48 (table S1). We assessed the fit of models incorporating the age and year parameters as 1) linear
49 parametric terms, 2) smoothing terms fitted using thin plate regressions splines (Wood 2003), 3)
50 separate smoothing terms for wild-caught and captive-born females, to capture the interaction
51 between age/year and birth origin, and 4) a tensor product interaction smoothing term, with
52 separate terms for wild-caught and captive-born females, to capture the interaction between all
53 explanatory variables (Wood 2006). Finally, we also explored the fit of models incorporating a
54 linear term for population size in each year, to assess density dependence in life-history traits and
55 whether there was a need to incorporate density dependence in future projections. All models
56 also had a linear parametric term for birth origin, to assess the differences in mean vital rates
57 between wild-caught and captive-born females. Although a previous study found an effect of the
58 time in captivity on survival in this population (Lahdenperä et al. 2018), because we aimed to
59 assess population viability without continued wild capture (after 1995) this was not included in our
60 model selection. All models also had a random effect smoothing term of spatial division group in
61 Myanmar, penalized with a ridge penalty. We had life history records from 11 out of 14 spatial
62 divisions (Ayeyarwady = 878, Bago = 7167, Chin = 1066, Kachin = 7252, Magway = 3322,
63 Mandalay = 11650, Rakhine = 2004, Sagaing = 25713, Shan = 5749, Tanintharyi = 142, Yangon
64 = 356, Unknown= 4984; figure S1). In the analyses, to make sample sizes more comparable we
65 grouped divisions by proximity and elevation: Ayeyarwady, Yangon, Bago, Rakhine, and
66 Tanintharyi regions were all grouped together because of low sample size and their coastal
67 locations. Chin and Shan regions were grouped together because of their similar elevation and
68 low sample sizes. Finally, Magway and Mandalay regions were grouped together because of
69 similar altitude, proximity and low sample size. The best-fit models were selected using the Akaike

70 information criterion (AIC), and where the difference in AIC between the two best models was
71 less than 2, the simpler model with fewer interactions was selected (Akaike 1987, Burnham and
72 Anderson 2004).

73

74



75

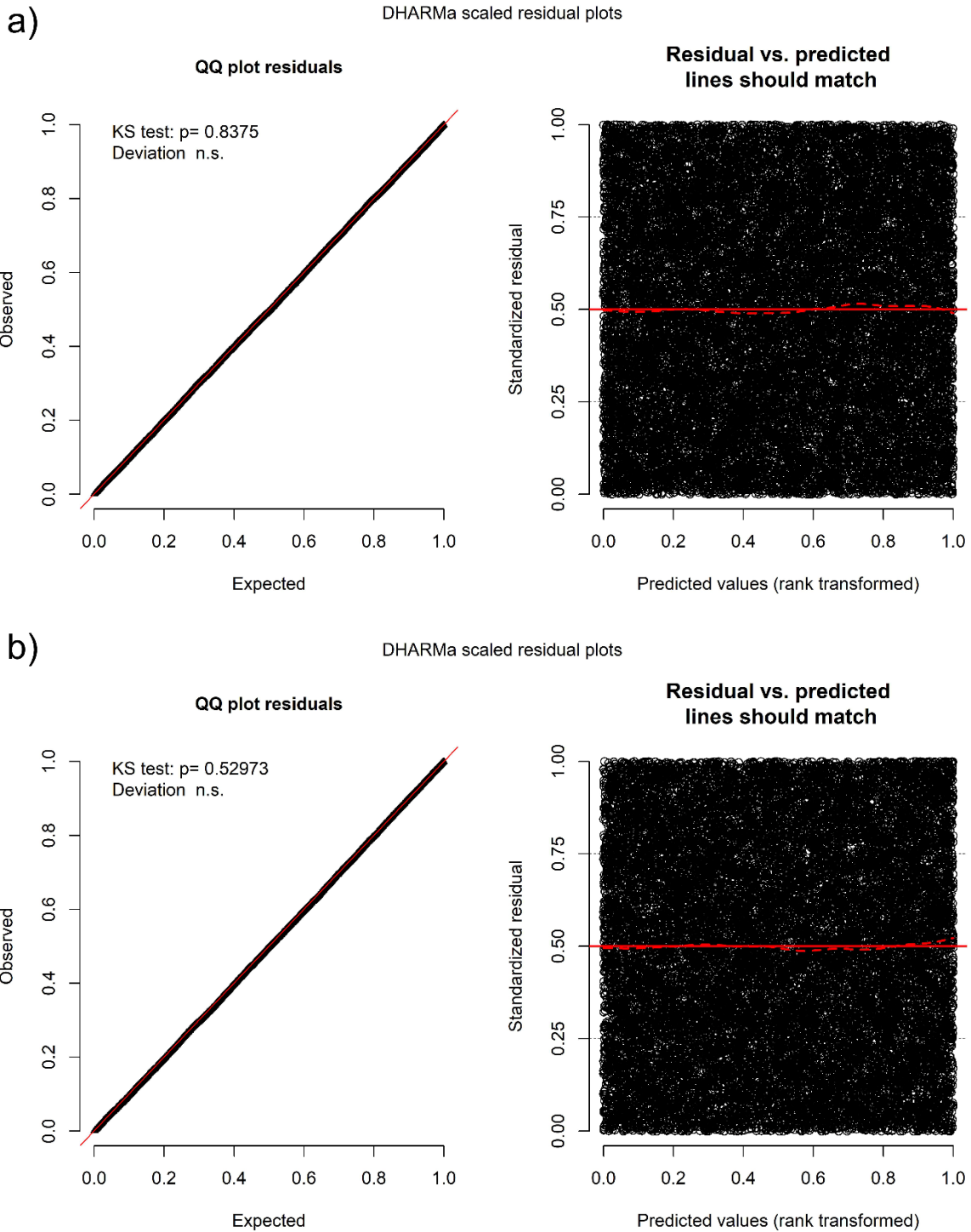
76 **Figure S1.** Regional divisions of Myanmar used in the current study. Colour denotes the regional
77 division groups used in analysis.

78

79

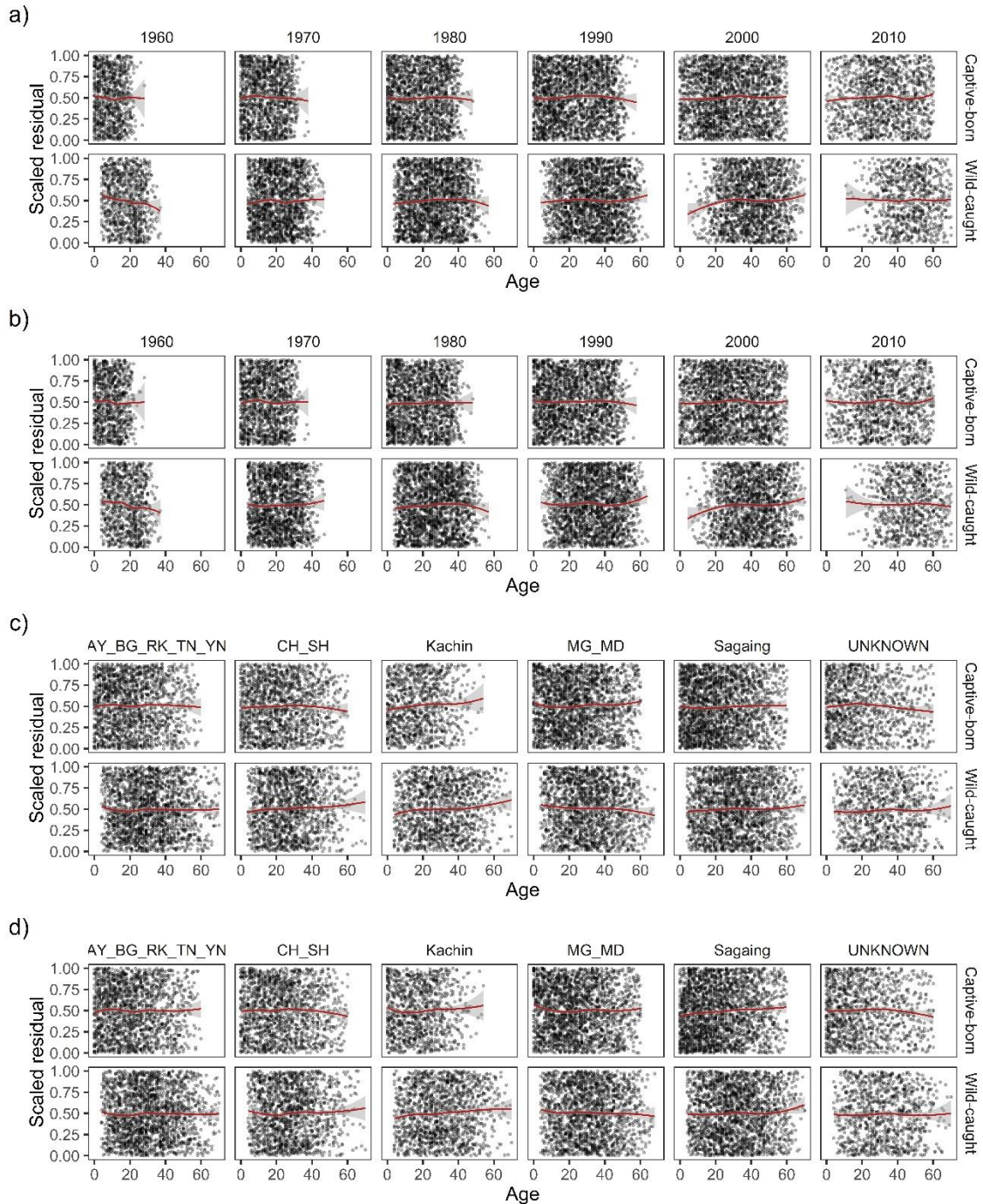
80 **Table S1.** Model selection results for age-specific life-history traits through time in female timber
81 elephants. Best model highlighted in bold. All models also included a binary response variable of
82 birth or mortality, a parametric term for birth origin, and an additional random effect smoothing
83 term predictor for regional division. The function $f(x)$ describes a thin plate regression spline
84 smoother, the function $g(x)$ describes a tensor product interaction smoothing term fit with a thin
85 plate regression spline, and the function $re(x)$ described a random effect smoothing term
86 penalised with a ridge penalty. Terms without functions delineate parametric, linear predictors.

Birth model predictors	AIC	ΔAIC
$g(\text{age, year, birth origin} = \text{captive-born}) + g(\text{age, year, birth origin} = \text{wild-caught}) + re(\text{year factor})$	12712.61	
$g(\text{age, year, birth origin} = \text{captive-born}) + g(\text{age, year, birth origin} = \text{wild-caught}) + \text{population size} + re(\text{year factor})$	12713.03	0.42
$f(\text{year, birth origin} = \text{captive-born}) + f(\text{year, birth origin} = \text{wild-caught}) + f(\text{age, birth origin} = \text{captive-born}) + f(\text{year, birth origin} = \text{wild-caught}) + re(\text{year factor})$	12732.73	20.12
$g(\text{age, year, birth origin} = \text{captive-born}) + g(\text{age, year, birth origin} = \text{wild-caught})$	12758.12	45.51
$f(\text{year, birth origin} = \text{captive-born}) + f(\text{year, birth origin} = \text{wild-caught}) + f(\text{age}) + re(\text{year factor})$	12759.73	47.12
$f(\text{year}) + f(\text{age, birth origin} = \text{captive-born}) + f(\text{year, birth origin} = \text{wild-caught}) + re(\text{year factor})$	12764.91	52.31
$f(\text{year, birth origin} = \text{captive-born}) + f(\text{year, birth origin} = \text{wild-caught}) + f(\text{age, birth origin} = \text{captive-born}) + f(\text{year, birth origin} = \text{wild-caught})$	12768.62	56.01
$f(\text{year, birth origin} = \text{captive-born}) + f(\text{year, birth origin} = \text{wild-caught}) + f(\text{age})$	12795.52	82.92
$f(\text{year}) + f(\text{age, birth origin} = \text{captive-born}) + f(\text{year, birth origin} = \text{wild-caught})$	12800.55	87.94
$f(\text{year}) + f(\text{age})$	12863.94	151.34
Half-decade + $f(\text{age})$	12872.52	159.91
Decade + $f(\text{age})$	12952.38	239.77
year + $f(\text{age})$	12987.26	274.65
year + age + year: age	13958.57	1245.96
$f(\text{year}) + \text{age}$	14204.45	1491.84
year + age + age: birth origin	14375.57	1662.96
year + age + year: birth origin	14414.02	1701.41
year + age	14415.25	1702.64
Mortality model predictors		
$g(\text{age, year, birth origin} = \text{captive-born}) + g(\text{age, year, birth origin} = \text{wild-caught}) + re(\text{year factor})$	8807.11	
$g(\text{age, year, birth origin} = \text{captive-born}) + g(\text{age, year, birth origin} = \text{wild-caught}) + \text{population size} + re(\text{year factor})$	8807.49	0.38
$f(\text{year, birth origin} = \text{captive-born}) + f(\text{year, birth origin} = \text{wild-caught}) + f(\text{age, birth origin} = \text{captive-born}) + f(\text{year, birth origin} = \text{wild-caught}) + re(\text{year factor})$	8839.35	32.24
$f(\text{year}) + f(\text{age, birth origin} = \text{captive-born}) + f(\text{year, birth origin} = \text{wild-caught}) + re(\text{year factor})$	8844.44	37.33
$g(\text{age, year, birth origin} = \text{captive-born}) + g(\text{age, year, birth origin} = \text{wild-caught})$	8862.64	55.53
$f(\text{year, birth origin} = \text{captive-born}) + f(\text{year, birth origin} = \text{wild-caught}) + f(\text{age}) + re(\text{year factor})$	8873.19	66.07
$f(\text{year, birth origin} = \text{captive-born}) + f(\text{year, birth origin} = \text{wild-caught}) + f(\text{age, birth origin} = \text{captive-born}) + f(\text{year, birth origin} = \text{wild-caught})$	8883.63	76.52
$f(\text{year}) + f(\text{age, birth origin} = \text{captive-born}) + f(\text{year, birth origin} = \text{wild-caught})$	8886.88	79.77
$f(\text{year, birth origin} = \text{captive-born}) + f(\text{year, birth origin} = \text{wild-caught}) + f(\text{age})$	8916.00	108.89
Hal-decade + $f(\text{age})$	8930.60	123.49
$f(\text{year}) + f(\text{age})$	8936.67	129.56
Decade + $f(\text{age})$	8947.66	140.55
year + $f(\text{age})$	9004.32	197.21
year + age + year: age	9480.85	673.74
year + age + age: birth origin	9515.23	708.12
$f(\text{year}) + \text{age}$	9526.44	719.33
year + age + year: birth origin	9581.47	774.36
year + age	9583.10	775.99

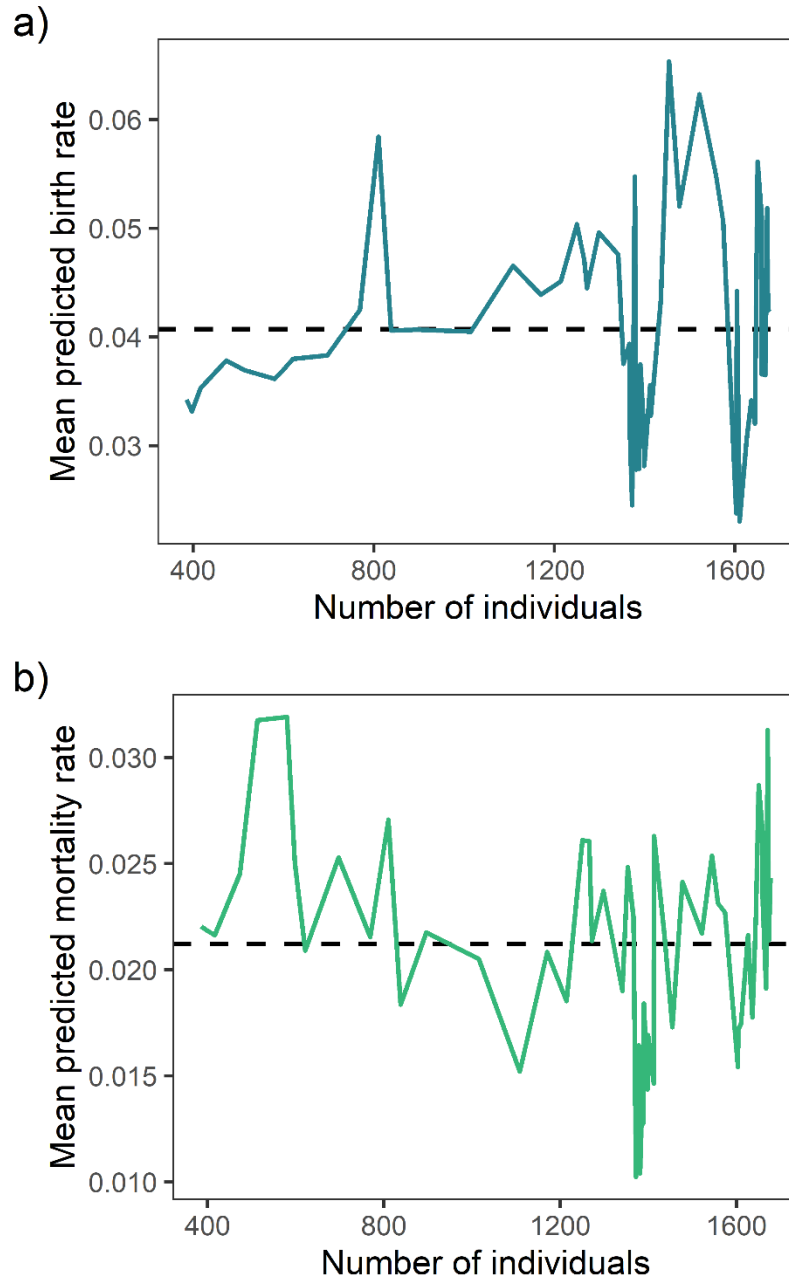


88

89 **Figure S2.** Scaled model residual diagnostics for the best-fit birth (a) and mortality (b) models
 90 over 1000 simulations. In neither birth nor mortality models was there evidence for deviation from
 91 uniformity in the residuals (left), or a relationship between predicted values and residuals (right).

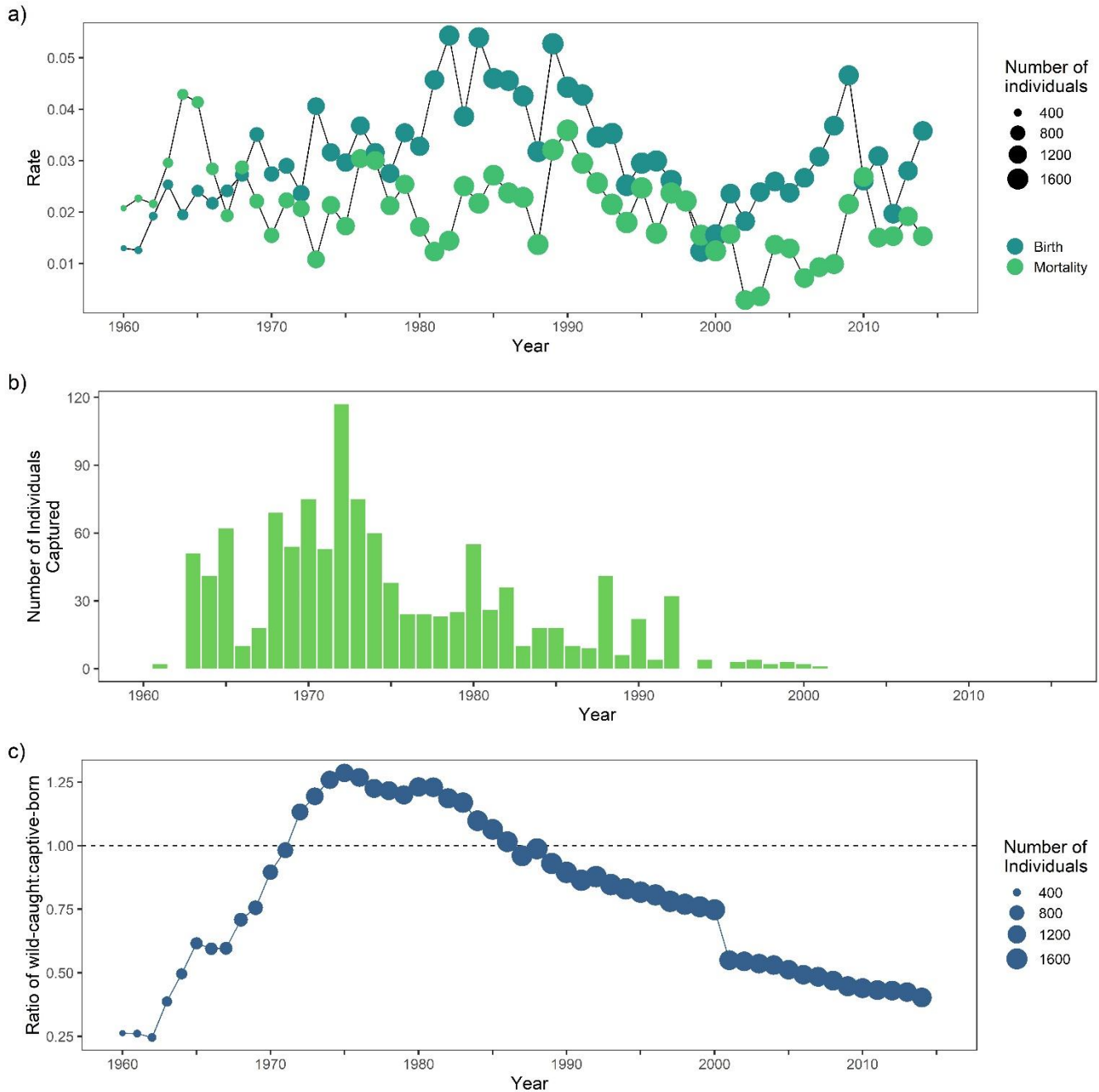


92 **Figure S3.** Scaled model residual covariance plots for the best-fit birth (a and c) and mortality (b
 93 and d) models. Scaled, simulated residuals were assessed against age, birth origin, decade (a
 94 and b) and regional division (c and d). Grouped regional division abbreviations: AY - Ayeyarwady,
 95 YN- Yangon, BG - Bago, RK- Rakhine, and TN- Tanintharyi, CH- Chin, SH-Shan, MG- Magway,
 96 MD- Mandalay. Points are scaled residuals, red lines are loess (localised regression) smoothers.

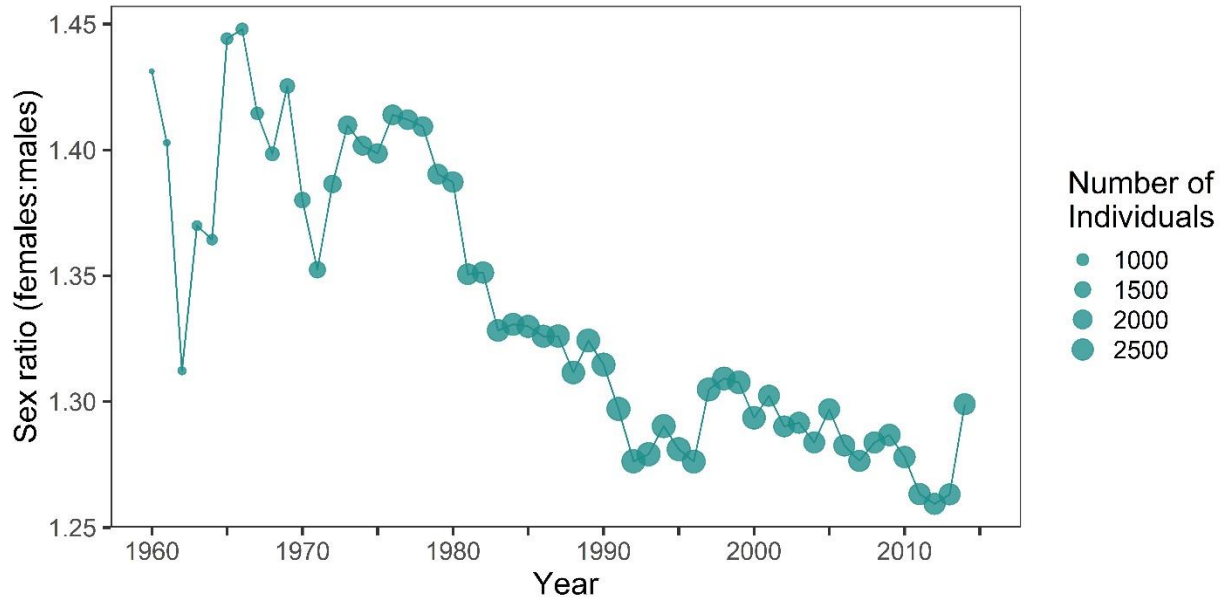


97

98 **Figure S4** – Mean model predicted values for the best-fit birth (a) and mortality (b) models with
 99 respect to population size. Solid lines are mean predicted vital rates, dashed lines are the mean
 100 birth and mortality rates across the study period. We found no clear relationship between
 101 population size and age-specific vital rates, and no further explanatory power when population
 102 size was included in the model (table S1).



103 **Figure S5.** Population trends in female timber elephants between 1960 and 2014. a) Raw annual
 104 birth and mortality rates for female timber elephants. The size of the points indicates the
 105 population size in each year (range = 385 - 1677). b) Annual capture rate estimates of wild female
 106 Asian elephants under the age of 25 in Myanmar between 1960 and 2014. c) The ratio of wild-
 107 caught females to captive-born females, where the size of the point indicates the population size
 108 (range = 385-1677).



109

110 **Figure S6.** Temporal trend in the sex ratio of timber elephants between 1960 and 2014. The size
111 of the points indicates the population size (range = 654-2991).

112

113

114

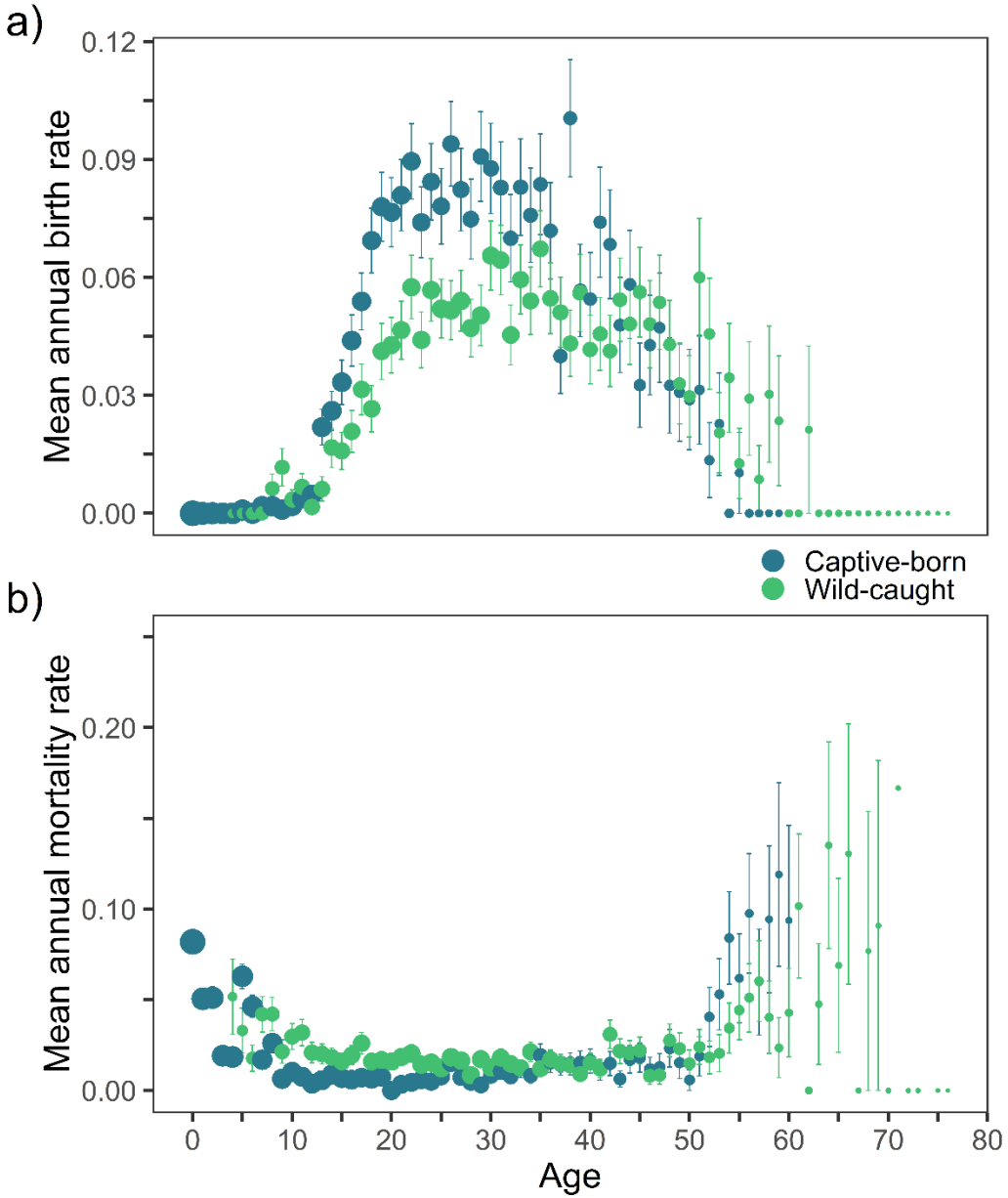
115

116

117

118

119

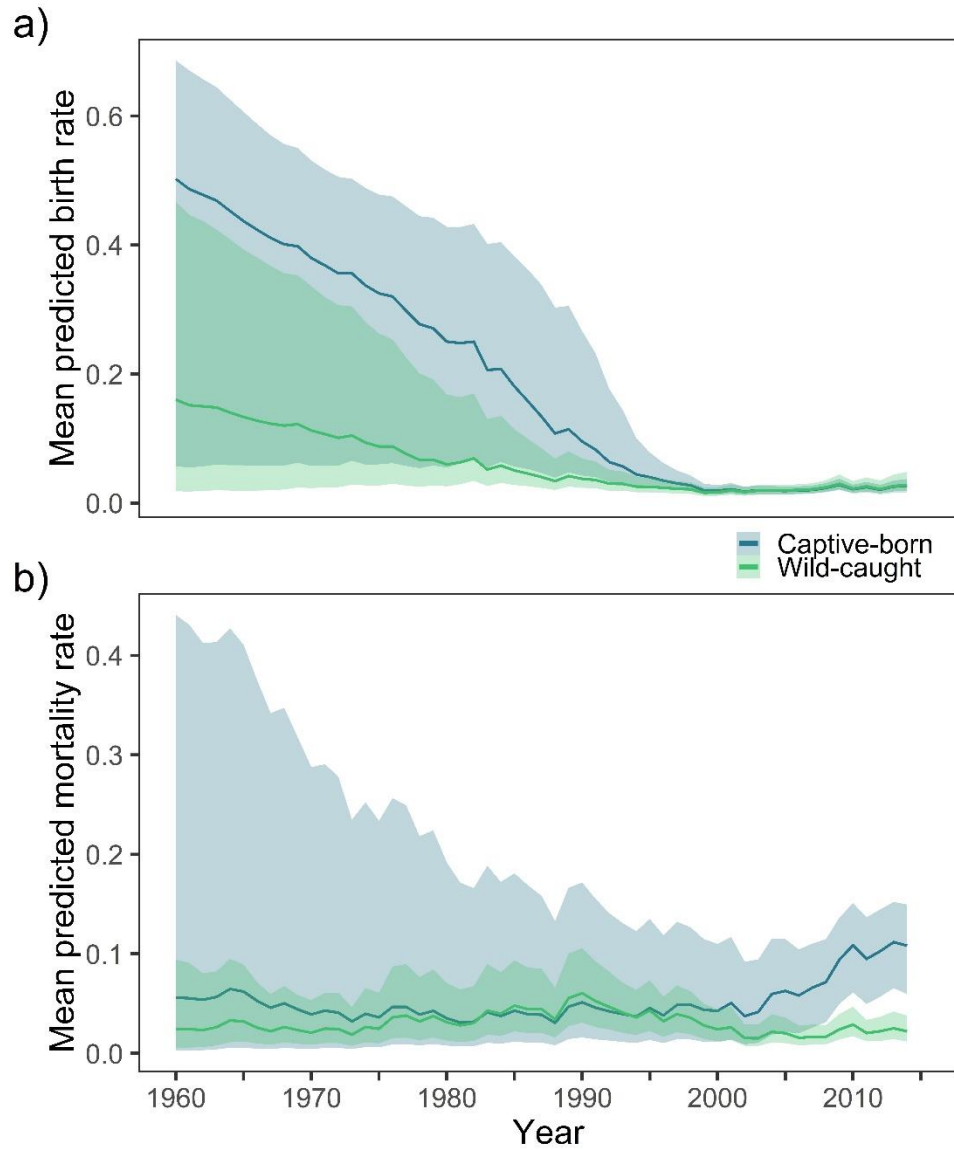


120

121 **Figure S7.** Mean age-specific birth (a) and mortality (b) rates in captive-born and wild-caught
 122 female timber elephants between 1960 and 2014. Points are mean annual age-specific birth rates
 123 across all years and regional divisions in Myanmar, with standard error bars. The size of the points
 124 indicates the sample size for a given age (range = 1-1965).

125

126



127

128 **Figure S8.** Change in the mean predicted birth (a) and mortality (b) rates between 1960 and 2014
 129 for captive-born and wild-caught females. Lines are mean model predicted values over 1000
 130 posterior simulations with 95% confidence intervals.

131

132

133

134 **S3. Formulation of the stochastic individual-based model**

135 Description of the individual-based model using the ODD protocol described by Grimm et al. 2006.

136 *S3.1 Purpose*

137 The purpose of the model is to understand the long-term population dynamics of captive female
138 elephants in Myanmar in a scenario where wild-capture is no longer practised. Here we present
139 only the formation of the first age-specific projection model, which incorporated only demographic
140 stochasticity and the mean age-specific birth/mortality probabilities across study years (1995-
141 2014) for each birth origin.

142 *S3.2 State variables and scales*

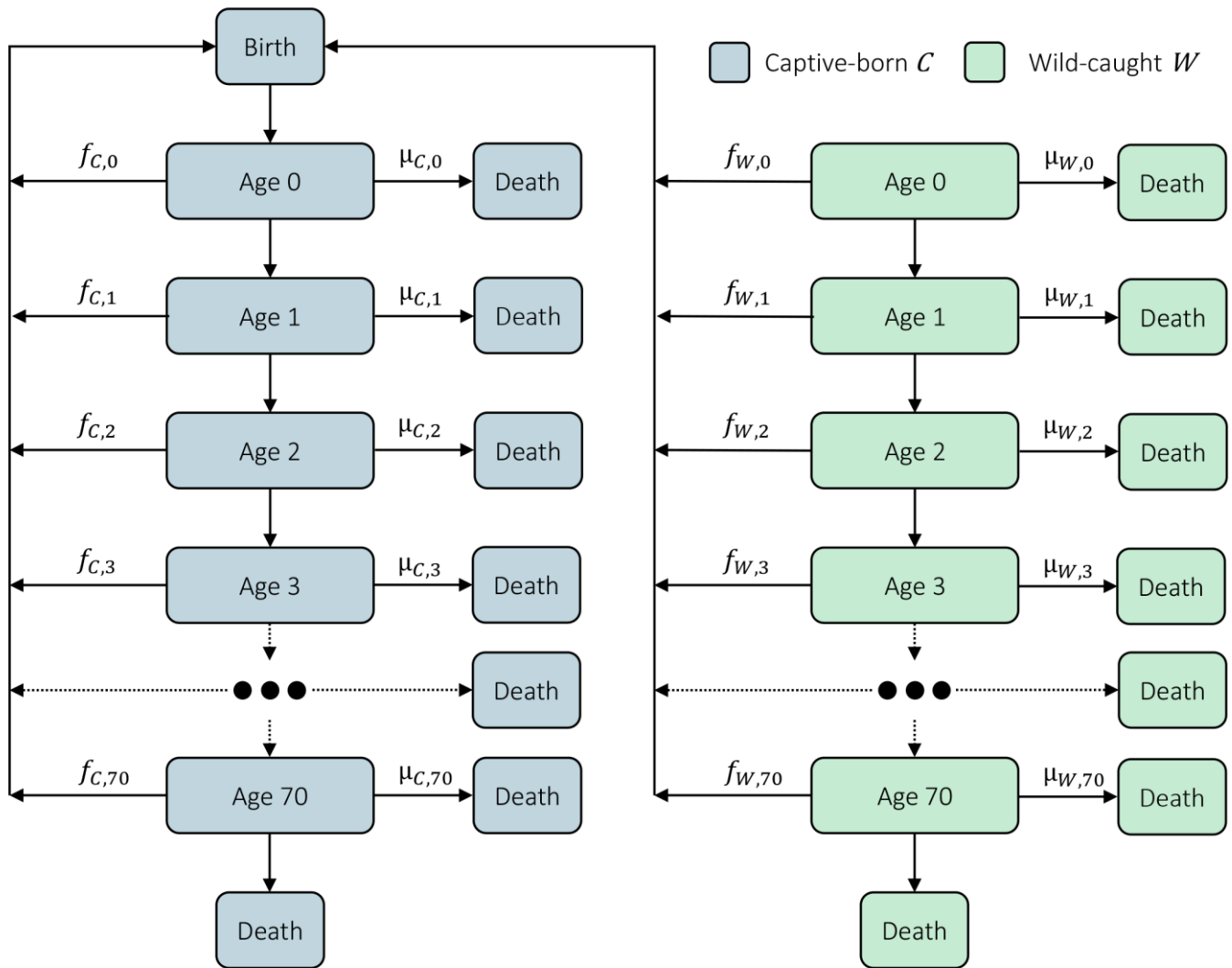
143 The model is formed at the level of each individual female. Individuals are characterised by two
144 state variables: Their age (a , integer between 0 and 70 in years) and their birth origin (captive-
145 born C , or wild-caught W). The population is characterised by the number of individuals in a given
146 year (at each age and of each birth origin).

147 *S3.3 Process overview and scheduling*

148 The model proceeds in annual time steps. Within each year or time step, 2 phases are processed
149 in the following order: birth and mortality. This order was selected in order to allow females to
150 reproduce and die in the same year. In each year, based on their age and birth-origin, females
151 had a given probability of reproduction or mortality. An overview of the life-cycle and transition
152 probabilities is given in figure S9.

153

154



155

156 **Figure S9.** A schematic of the life-cycle for the individual-based stochastic projection model for
 157 female timber elephants without wild-capture. Colour denotes birth origin. Each individual at each
 158 age (a) had mean annual predicted birth probabilities of $f_{C,a}$ (captive-born) and $f_{W,a}$ (wild-caught),
 159 and mean annual predicted mortality probabilities of $\mu_{C,a}$ (captive-born) and $\mu_{W,a}$ (wild-caught).
 160 All individuals born were captive-born females at age 0. Individuals living past the age of 70 were
 161 removed from the analysis.

162

163 S3. 4 Design concepts

164 Stochasticity: Birth and mortality are interpreted as binary events drawn from the Bernoulli
165 distribution for each individual from each birth origin, with a probability from the mean age-specific
166 probability from the best-fit birth and mortality models. Observation: For model analysis, we
167 recorded the population-level variable of $\ln population\ size$.

168 S3. 5 Initialization and input

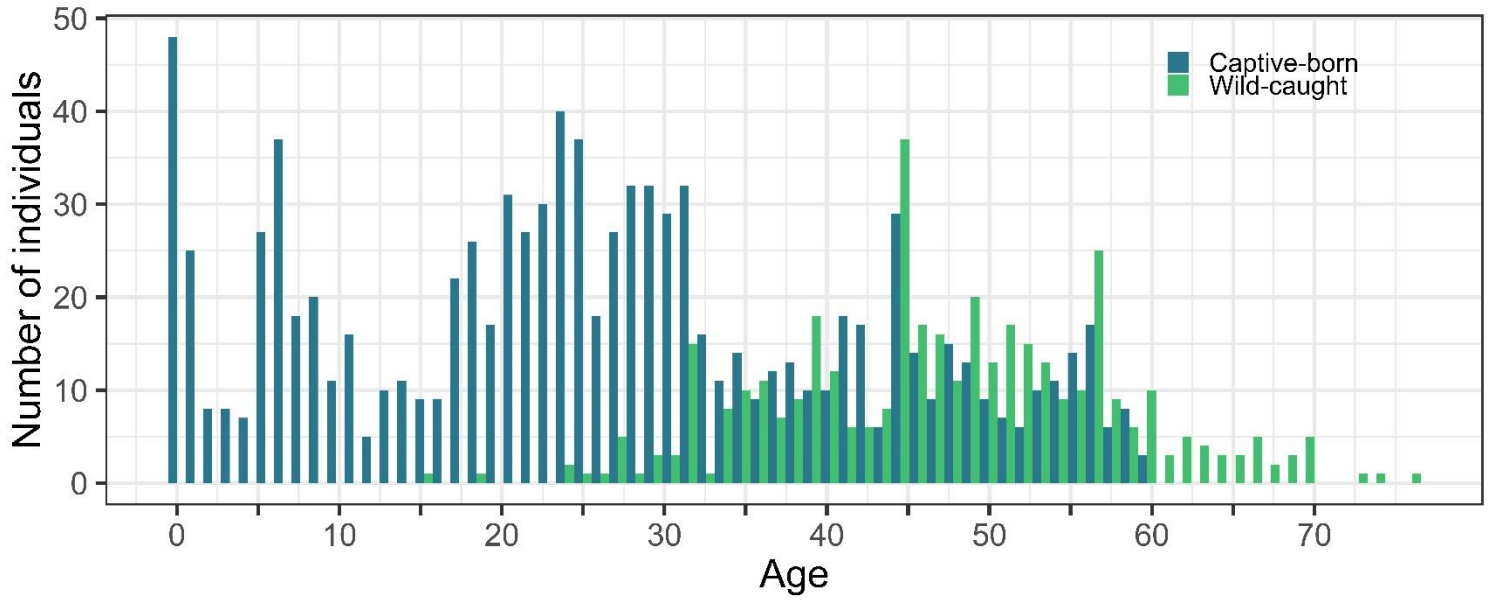
169 We began the projection with the age-structure present in 2014 (N = 1369), which had 976
170 captive-born females and 393 wild-caught females. The starting age-structure is given in figure
171 S11. Demographic stochasticity was incorporated by performing 500 iterations of the projection
172 model. We projected forward 250 years, which captured long-term trends over 10-12.5
173 generations. For this projection, age-specific birth and mortality probabilities were averaged
174 across the study period (1995-2014) from the best-fit model predictions. Furthermore, the
175 projection was run on predicted values from the Kachin regional division. Explicitly, the mean age-
176 specific predicted birth probability, $p(birth)$, is given by the following binomial additive model

177
$$p(birth) = [1 + e^{-(\beta_0 + g(a, C) + g(a, W))}]^{-1}$$

178 Where β_0 is the intercept, and the function $g()$ describes a tensor product interaction smoothing
179 term fit with a thin plate regression spline for an individual at age a , and separately for captive-
180 born, C , and wild-caught, W , females, but averaged across years 1995-2014, rather than
181 incorporating an observation year effect (table S1). The mean age-specific predicted mortality
182 probability, $p(mort)$, is given by the following binomial additive model

183
$$p(mort) = [1 + e^{-(\beta_0 + g(a, C) + g(a, W))}]^{-1}.$$

184



185

186 **Figure S10.** A histogram of the starting age-structure for stochastic, individual-based population
 187 projections, which was the age-structure present in 2014 (N = 1369). Ages are in 1-year bins.
 188 Colour denotes the birth origin.

189

190

191

192

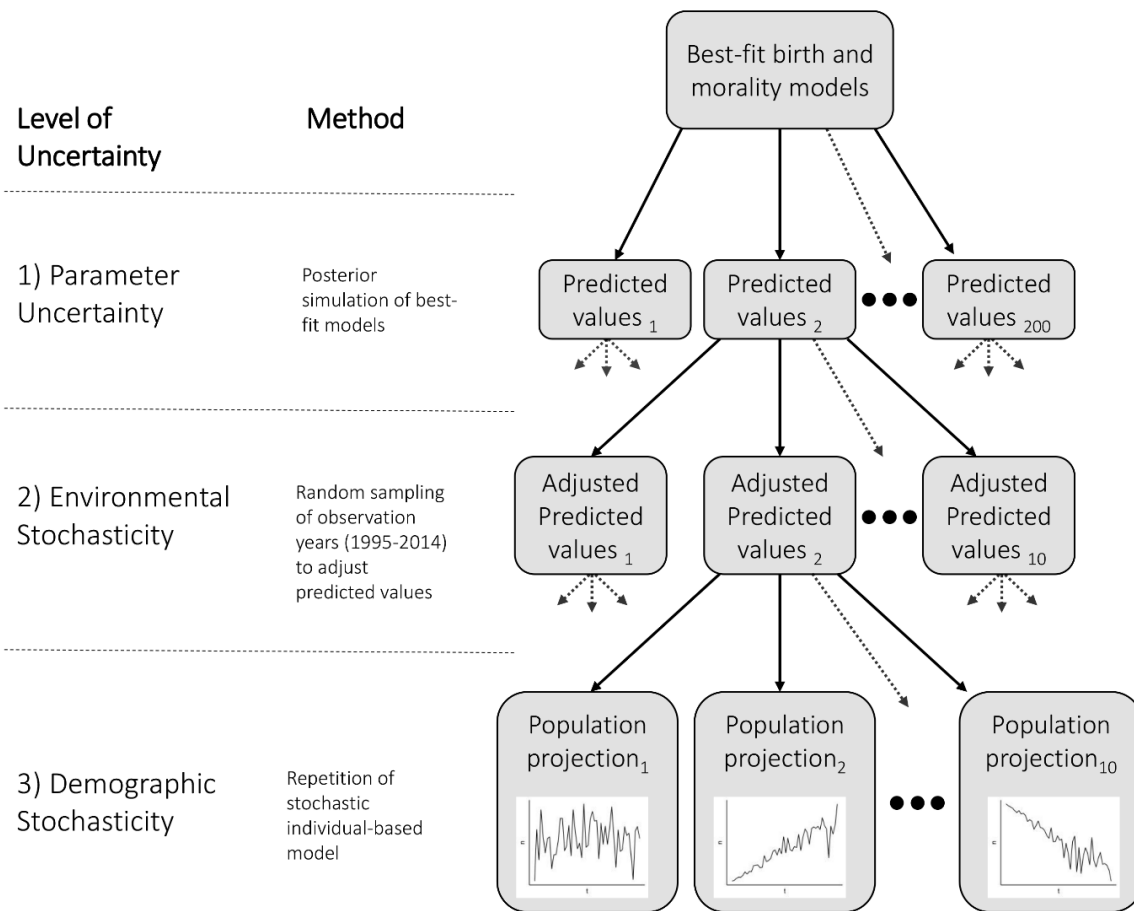
193

194

195

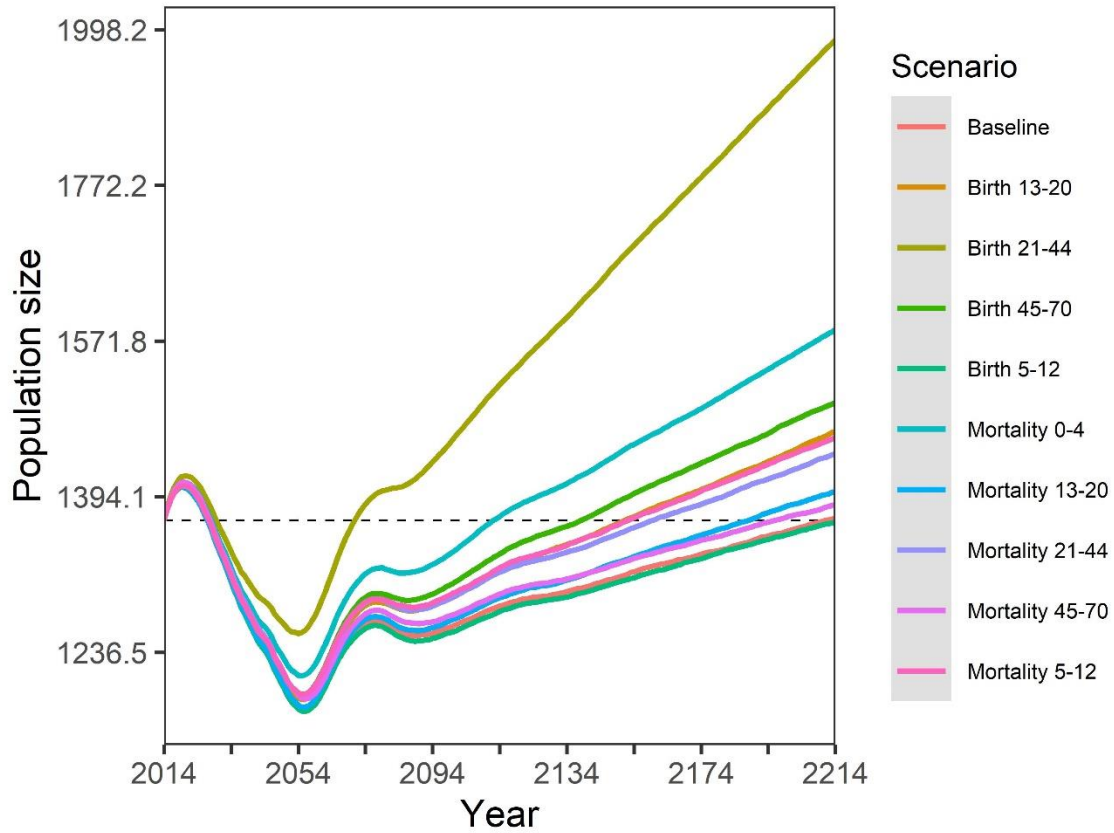
196

197



198

199 **Figure S11.** A schematic of the simulation framework for implementing the hierarchical population
 200 viability analysis under different levels of uncertainty. Starting from the best-fit birth and mortality
 201 models, 1) parameter uncertainty was incorporated through posterior simulation, generating 200
 202 sets of predicted values. 2) Environmental stochasticity was incorporated by randomly sampling
 203 10 sets of years (1995-2014) and adjusting predicted values based on observed variation in those
 204 years. 3) Demographic stochasticity was incorporated by repeating each population projection 10
 205 times. When partitioning the variance in $\ln population\ size$ to these three levels of uncertainty, for
 206 each year we incorporated the hierarchical framework of demographic stochasticity within
 207 environmental stochasticity within parameter uncertainty using nested intercept-only random
 208 effects.



209

210 **Figure S12.** All scenarios of demographic change and their influence on population viability over
 211 200 years. Each line represents either the baseline, average scenario of long-term viability or a
 212 scenario with a 10% increase (birth rates) or 10% decrease (mortality rates) for specific age
 213 classes. Population size axis on the natural logarithmic scale, dashed line represents starting
 214 population size.

215

216

217

218